energies

MDPI

Article

Design of a More Efficient Rotating-EM Energy Floor with Lead-Screw and Clutch Mechanism

Thitima Jintanawan [1], Gridsada Phanomchoeng [1,2,*], Surapong Suwankawin [3], Weeraphat Thamwiphat [1], Varinthorn Khunkiat [1] and Wasu Watanasiri [1]

[1] Department of Mechanical Engineering, Chulalongkorn University, Bangkok 10330, Thailand
[2] Micro/Nano Electromechanical Integrated Device Research Unit, Faculty of Engineering, Chulalongkorn University, Bangkok 10330, Thailand
[3] Department of Electrical Engineering, Chulalongkorn University, Bangkok 10330, Thailand
* Correspondence: gridsada.phanomchoeng@gmail.com; Tel.: +66-2-218-6630

Abstract: There is an interest in harvesting energy from people's footsteps in crowded areas to power smart electronic devices with low consumption. The average power consumption of these devices is approximately 10 μW. The energy from our footsteps is green and free, because walking is a routine activity in everyday life. The energy floor is one of the most efficient pieces of equipment in vibration-based energy harvesting. The paper aims to improve the previous design of the energy floor—called Genpath—which uses a rotational electromagnetic (EM) technique to generate electricity from human footsteps. The design consists of two main parts of (1) the EM generator, including the lead-screw mechanism for translation-to-rotation conversion, and (2) the Power Management and Storage (PMS) circuit. The improvement was focused on the part of the EM generator. A thorough investigation of the design components reveals that the EM generator shaft in the previous Genpath design cannot continuously rotate when the floor-tile reaches the bottom end, resulting in no energy gain. Therefore, a one-way clutch is implemented to the system to disengage the generator shaft from the lead-screw motion when the floor-tile reaches the allowable displacement. During the disengagement, the EM generator shaft still proceeds with a free rotation and could generate more power. In our analysis, the dynamic model of the electro-mechanical systems with the one-way clutch was successfully developed and used to predict the energy performances of the VEH floors and fine-tune the design parameters. The analytical result is shown that the spring stiffness mainly affects the force transmitted to the EM generator, and then the induced voltage and power of the generator, thus, the value of the stiffness is one of the critical design parameters to optimize. Finally, the new prototype consisting of 12-V-DC generator, mechanisms of lead-screw and clutch, as well as coil springs with the optimal stiffness of 1700 N/m was built and tested. The average energy produced by the new prototype is 3637 mJ (or average power of 3219 mW), per footstep which is 2935 mJ greater than that of the previous design. Moreover, to raise the social awareness about energy usage, the sets of Genpath have been used to organize an exhibition, "Genpath Empower our Journey". The people who stroll forward on the paths can realize how much energy they gain from their footsteps.

Keywords: energy harvesting; electromagnetic generator; energy floor tile; power management system; footstep energy harvesting; piezoelectric; energy harvesting paver; clutch

Citation: Jintanawan, T.; Phanomchoeng, G.; Suwankawin, S.; Thamwiphat, W.; Khunkiat, V.; Watanasiri, W. Design of a More Efficient Rotating-EM Energy Floor with Lead-Screw and Clutch Mechanism. *Energies* **2022**, *15*, 6539. https://doi.org/10.3390/en15186539

Academic Editors: Hassen M. Ouakad and Issam M. Bahadur

Received: 8 August 2022
Accepted: 4 September 2022
Published: 7 September 2022

1. Introduction

In recent decades, the Internet of things (IoT) has caused technological evolution not only in industries or factories, but also in household life. The IoT technology found in the present products such as smart phones, smart watch, IoT sensors, Global Positioning System (GPS) tracking, data acquisition system (DAQ) system, and wireless devices has been involved in most residential, educational, medical and industrial sectors [1,2]. Consequently, more electrical power sources are needed to operate such increasing industrial and

household products. The power needs of mobile devices such as smart watches, RFID, or MEMS sensors varies from few microwatts to hundreds of milliwatts for mobile phone or GPS applications, but most devices are usually in a sleep mode for 99.9% of their operation time. They wake up for a few milliseconds only to communicate data. Despite this, the advanced technology makes each product requires only a low power supply because the average power consumption of these devices is approximately 10 μW [3]. There are more than 14.4 billion IoT devices requiring power in 2022 and there will be 27.0 billion devices more in 2025 [4,5]. The world's demand of electrical power has been rapidly growing!

With the wireless fourth/fifth-generation (4G/5G) of cellular network technology, the current IoT products are convenient for mobile use and are capable of working 7 days and 24 h. The continuity requirement makes the battery technology one of the key features of the products [6]. However, battery lifespan and charging seem to be issues of the power source. Therefore, energy harvesting is attracting attention as "enabling technology" to expand the IoT utilization and enhance life and social resilience [7–9]. Energy harvesting utilizes the ambient energy present in the environment by converting them into electrical energy and using them as a remote power source for the autonomous electronic devices or circuits. The ambient energy may come from heat, electromagnetic, wind, solar power, and vibration [10–15]. Moreover, vibration-based energy from human movement is currently one of the most interesting sources for harvesting and being used as a remote power source [16,17].

For the vibration-based energy harvesting from people's footsteps, walking is a normal activity that everyone does every day. The heel strike of a person's walk can generate energy of 2–20 watts or power of 1–5 joules per step [18]. The energy from people walking is green and free. If a simple calculation is performed based on the prediction of more than 21 trillion walking steps per day [19,20], and all of energy from the walking steps could be ideally harvested, one can imagine how much energy is obtained. There are some commercial products which can harvest energy from human walking such as energy storage shoes and the energy floor [21–24]. Pavegen and Energy Floors have produced a commercial system that generates power from footsteps [22,23]. The electromagnetic generator system of Pavegen can generate energy of 2 to 4 joules, or around 5 watts of power of off-grid electrical energy per step, while Energy Floors focuses on converting humans dancing and playing games to electrical energy. However, there are few technical details of those products published thus far.

To harvest energy from human walking, a Vibration Energy Harvesting (VEH) system called Genpath, the smart floor capable of conversing kinetic energy from thousands, has been developed [24,25]. It can be installed in places where crowds of people walk to harvest energy. Genpath in [24,25] utilized the lead screw or rack-pinion mechanism to convert the translation of the floor-tile to the rotation of the electromagnetic (EM) generator to induce voltage when the force from a footstep is applied. Then, the electrical voltage and power generated by the EM generator are processed by the connected Power Management and Storage (PMS) circuit. The harvested power is then stored in the rechargeable batteries. The power from the battery can be supplied to the smart IoT-devices with low energy consumption. Ref. [24] reports that the Genpath prototype-II or Genpath V1 produces an average energy of up to 702 mJ (or average power of 520 mW) per footstep.

However, a thorough investigation of the design components as well as the dynamics of the Genpath system reveals that it can be improved for a more efficient design. The Genpath V1 design still has limitations described as follows. The major limitation of Genpath V1 is that the EM generator shaft cannot continuously rotate when the floor-tile moves to the bottom end. When the EM generator shaft is stopped, the EM generator cannot generate energy. Moreover, the spring stiffness of Genpath affects the force transmitted to the EM generator and also the induced voltage and power. To optimize the spring stiffness is also necessary.

Therefore, the objective of the paper is to present a more efficient design of vibration-based energy harvesting (VEH) floor. Based on the design of Genpath V1, the VEH floor

embedded with the rotational electromagnetic (EM) generator, the key concept of the new design is to use the one-way clutch to disengage the rotation of the generator shaft from the lead screw and bevel gear during the restoring period, allowing the generator to continue its free rotation and thus gain more energy. In addition, with the clutch disengagement, the frictional resistance on the mechanical side of the movement converter can be reduced, allowing the implement of the softer spring in the design to increase the maximum speed and also the induced voltage peak of the generator. Consequently, the new design of the energy floor with the clutch and the softer springs is much more efficient than the previous design. To achieve this purpose, the dynamic models of the electro-mechanical systems with a one-way clutch were developed using MATLAB®/Simulink for predicting the energy performance of the VEH floors, and the dynamic models were used to fine-tune the design parameters. The entire system consists of two main parts: (1) the EM generator, including the translation-to-rotation conversion mechanism, and (2) the Power Management and Storage (PMS) circuit. For simplicity, a direct-current (DC) generator was used in the design to produce electricity. The lead-screw mechanisms were adopted to converse a linear motion from a human's pedal to a rotation of the generator's rotor. The PMS circuit with extra low energy consumption was designed to simultaneously convert and store electrical energy. The paper is organized into the following sections. In Section 2, the conceptual design of the system is described in detail. Then the model and analysis parameters are presented in Section 3. Next, the Genpath V2 prototype and its test results are presented in Section 4. Further, the power management system of the Genpath is presented in Section 5. The installation and demonstration of application are presented in Section 6. Finally, the conclusion is stated in Section 7.

2. Conceptual Design

Recently, energy harvesting from human motion has become a common interest. The energy floor which harvests energy from human footsteps is applicable to crowded areas. The design of the energy floor using an electromagnetic generator is quite simple and efficient [22–25]. In the design, there exists a mechanism to convert a linear motion to a rotational motion to drive the generator. From the design of Genpath V1 [24], the lead screw and bevel gear were used to convert the motion. The bevel gear was then connected to the generator shaft to transmit the power. When the floor tile reaches the allowable displacement at the bottom end, the springs installed at the corners help restore the system back to its equilibrium. This electro-mechanical harvester [24] can generate an averaged energy of 702 mJ per footstep. However, there was a major flaw in the mechanism yet to be improved. Based on the profile of force [26] applied from a footstep and the corresponding harvested power/energy typically obtained from the previous design [24], respectively. For 0.7 s of footstep force applying, there is an interval which the harvester has no energy gain ~0.2 s, i.e., during 0.4–0.6 s, as observed in the results of [24]. It occurs when the floor-tile motion is limited by the allowable displacement of 15 mm, causing both the lead screw and the generator shaft ceased. Therefore, no electrical power is generated during 0.4–0.6 s. All the parts stay at rest until the combined restoring spring force and applied force can overcome the friction in the system, and then they are restored back to the initial position. There was also a limitation of spring tuning in the restoring period of the previous design. Theoretically, to harvest more energy, the softer spring with smaller value of coefficient is desirable [24]. However, the spring coefficient in the previous design [24] needs to be at least 20,000 N/m to overcome the system friction and be capable to restore the floor tile back.

A one-way clutch mechanism is proposed to solve the existing problems. A one-way clutch is a coupling machine element where its inner ring is only coupled and rotated with the outer ring in one direction but rotated freely in the opposite direction. The clutch is used to disengage the rotation of the generator shaft from the lead screw and bevel gear during the restoring period, allowing the generator to continue its free rotation and thus gain more energy. The schematic diagram in Figure 1a illustrates the design of the energy

floor with the one-way clutch mechanism. The clutch is assembled to the system through the customized housing as shown in Figure 1b. Additionally, the function of the one-way clutch mechanism is shown in Figure 1c.

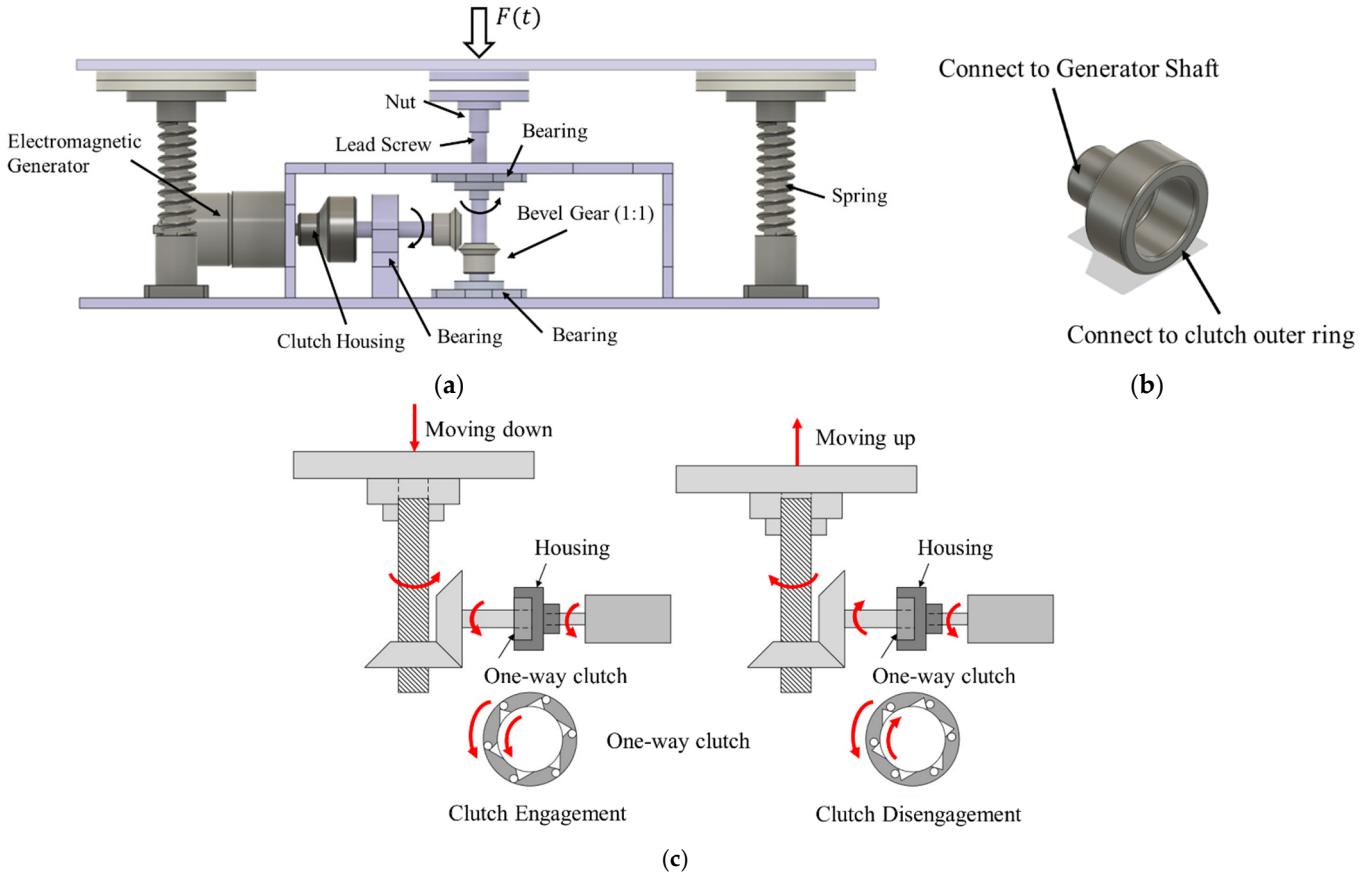

Figure 1. The design of kinetic-energy harvesting floor with the one-way clutch mechanism: (**a**) schematic diagram of Genpath V2 design; (**b**) clutch housing; (**c**) function of the one-way clutch mechanism.

In operation, the floor-tile first moves down due to the applied force from a footstep, causing the nut which is fixed to the tile center to move down and drive the lead screw to rotate about its axis. The lead screw's rotation is then transmitted to the DC generator through the bevel gear. The rotation of the generator shaft causes the induced voltage and hence the power to be harvested. When the floor tile reaches its allowable displacement of 15 mm and tends to restore back to the equilibrium position with spring forces, the lead-screw rotation starts to rotate in the opposite direction. Meanwhile, the clutch is disengaged, and the generator continues to rotate, but now freely, with its inertia.

3. Modeling and Analysis

In this section, the equations governing the electro-mechanical system with clutch design are presented. The equations governing both stages of the clutch engagement and disengagement were developed. Then, the harvested power/energy can be predicted using Matlab®/Simulink [27]. The developed analytical model is used for the parametric study where the parameter set could be optimized.

3.1. Governing Equations

For the clutch engagement stage, the equations governing the electro-mechanical system with the lead screw and clutch design are not different from those governing the

system without clutch. The interested reader can follow the detailed derivation from [24]. The equations are

$$\begin{bmatrix} \dot{i} \\ \dot{\theta} \\ \ddot{\theta} \end{bmatrix} = \begin{bmatrix} -\left(\frac{R_G + R_L}{L}\right) & 0 & \frac{K_t}{L} \\ 0 & 0 & 1 \\ -\frac{K_t}{J_{eq}\Delta} & 0 & \frac{-d_m}{J_{eq}\Delta} \end{bmatrix} \begin{bmatrix} i \\ \theta \\ \dot{\theta} \end{bmatrix} + \begin{bmatrix} 0 \\ 0 \\ \frac{F(t)-F_s}{J_{eg}} \end{bmatrix} \tag{1}$$

Or

$$\begin{bmatrix} \dot{i} \\ \dot{x} \\ \ddot{x} \end{bmatrix} = \begin{bmatrix} -\left(\frac{R_G + R_L}{L}\right) & 0 & \frac{K_t}{L} \\ 0 & 0 & 1 \\ -\frac{lK_t}{2\pi J_{eq}\Delta} & 0 & \frac{-ld_m}{2\pi J_{eq}\Delta} \end{bmatrix} \begin{bmatrix} i \\ x \\ \dot{x} \end{bmatrix} + \begin{bmatrix} 0 \\ 0 \\ \frac{l(F(t)-F_s)}{2\pi J_{eg}} \end{bmatrix} \tag{2}$$

where the state variables: i is the current, θ is the angular position of the lead screw and the bevel gear and $x = \frac{l\theta}{2\pi}$ is the displacement of the floor tile. Note that l is the pitch of the lead screw. Additionally, $F(t)$ is the footstep applied force and F_S is the restoring spring force. In (1) and (2), $J_{eq} = \frac{ml}{2\pi} + \frac{(J_1+J_G)}{\Delta}$ is the equivalent moment of inertia corresponding to the mass of the plate and nut m, and the mass moments of inertia of the lead screw and bevel gear J_1 and J_G, respectively. In addition, Δ is the adjusted coefficient according to the frictions in the power transmission, where $\Delta = \frac{l}{2\pi\eta_1\eta_2}$, with η_1 and η_2 are the efficiencies of the screw thread and the thrust bearing, respectively. The damping coefficient d_m in (1) and (2) is simply represented the viscous damping due to the friction in the bevel gear and the clutch. For the electrical side, K_t is the back emf (torque) constant, L is the inductance of the generator, R_G is the resistance of the generator and R_L is the resistance of the load and $F(t)$ is input force.

The instantaneous power from the generator when the load resistance is connected is then

$$P = i^2 R_L. \tag{3}$$

The averaged energy and averaged power harvested in one footstep can be determined, respectively, from

$$E = \int_0^T P dt, \tag{4}$$

$$P_{av} = \frac{E}{T}. \tag{5}$$

If the inductance L is negligible, (1) can be decoupled and simplified as

$$J_{eq}\ddot{\theta} + (c_m + c_e)\dot{\theta} + F_s = F(t), \tag{6}$$

and

$$i = \left(\frac{K_t}{R_G + R_L}\right)\dot{\theta}, \tag{7}$$

where c_m and c_e are mechanical damping and electrical damping, respectively, given by

$$c_m = \frac{d_m}{\Delta},\ c_e = \frac{K_t^2}{\Delta(R_G + R_L)}, \tag{8}$$

From [28], the optimized load resistance for the maximum power is then

$$R_L = R_G + \frac{K_t^2}{c_m}, \tag{9}$$

For the stage of clutch disengagement, the generator is rotated free with the initial conditions obtained from the final time of the engagement period. The governing Equations (1) is then simplified for the disengagement period as

$$\begin{bmatrix} \dot{i} \\ \dot{\theta} \\ \ddot{\theta} \end{bmatrix} = \begin{bmatrix} -\left(\frac{R_G+R_L}{L}\right) & 0 & \frac{K_t}{L} \\ 0 & 0 & 1 \\ -\frac{K_t}{J_G} & 0 & \frac{-d_{m0}}{J_G} \end{bmatrix} \begin{bmatrix} i \\ \theta \\ \dot{\theta} \end{bmatrix} + \begin{bmatrix} 0 \\ 0 \\ 0 \end{bmatrix}, \quad (10)$$

Note that when the clutch is disengaged, the terms of inertia and friction according to the lead screw and the bevel gear are omitted from (10). Additionally, the term d_{m0} in (10) is represented only the damping according to the friction in the clutch; hence $d_{m0} \ll d_m$.

3.2. Simulink Model of the Harvesting System with Clutch Design

Figure 2 shows the Matlab®/Simulink model of the electro-mechanical system with clutch design for energy harvesting, according to (1)–(6) and (10). First, the parameter set as shown in Table 1, mostly based on the previous design, Genpath V1 [24], was used for the simulation. Both the footstep force obtained from [26] and the half-sine force function, shown in Figure 3, were alternatively used as the applied force and input to the Simulink model. The half-sine force function is used to evaluate the simulation and experiment because during the experiment in the laboratory, the Genpath V2 is pushed by foot. Thus, the footstep force is similar to a half-sine wave. For verification, the induced voltage and current and the corresponding power and energy from the prediction and from the experiment were compared in Figure 4. The magnitudes and profiles of the analytical results agree well with those from the experiment. In Figure 4, the predicted voltage/current and power/energy according to the half-sine force input is however more accurate, because the footstep force applied in the test is probably different from the normal walk. In addition, close agreement of the analytical and experimental results of the harvested power/energy summarized in Table 2 gives us confidence on the further use of the analytical model for the parametric design in Section 3.3.

Table 1. Genpath V2 parameters.

Parameters	Value
Pitch of Lead Screw (l)	8 mm
Mass of Nut and Plate (m)	2.16 kg
Moment of Inertia of lead screw (J_l)	2.5536×10^{-6} kg·m^2
Moment of inertia of bevel gear (J_G)	8.6750×10^{-7} kg·m^2
Lead angle	30 degrees
Spring Coefficient (k)	18,000 N/m
Damping Coefficient (d)	11,000 N·s/m
Resistance of Generator (RG)	37 Ohm
Inductance (L)	3.6×10^{-3} H
Generator constant (K_t)	0.2903 Vs/rad
Resistance of Load (R_L)	30 Ohm
Friction coefficient (μ)	0.21
Efficient of thrust bearing η_{thrust}	0.8101
Efficient of thread η_{thread}	0.6444

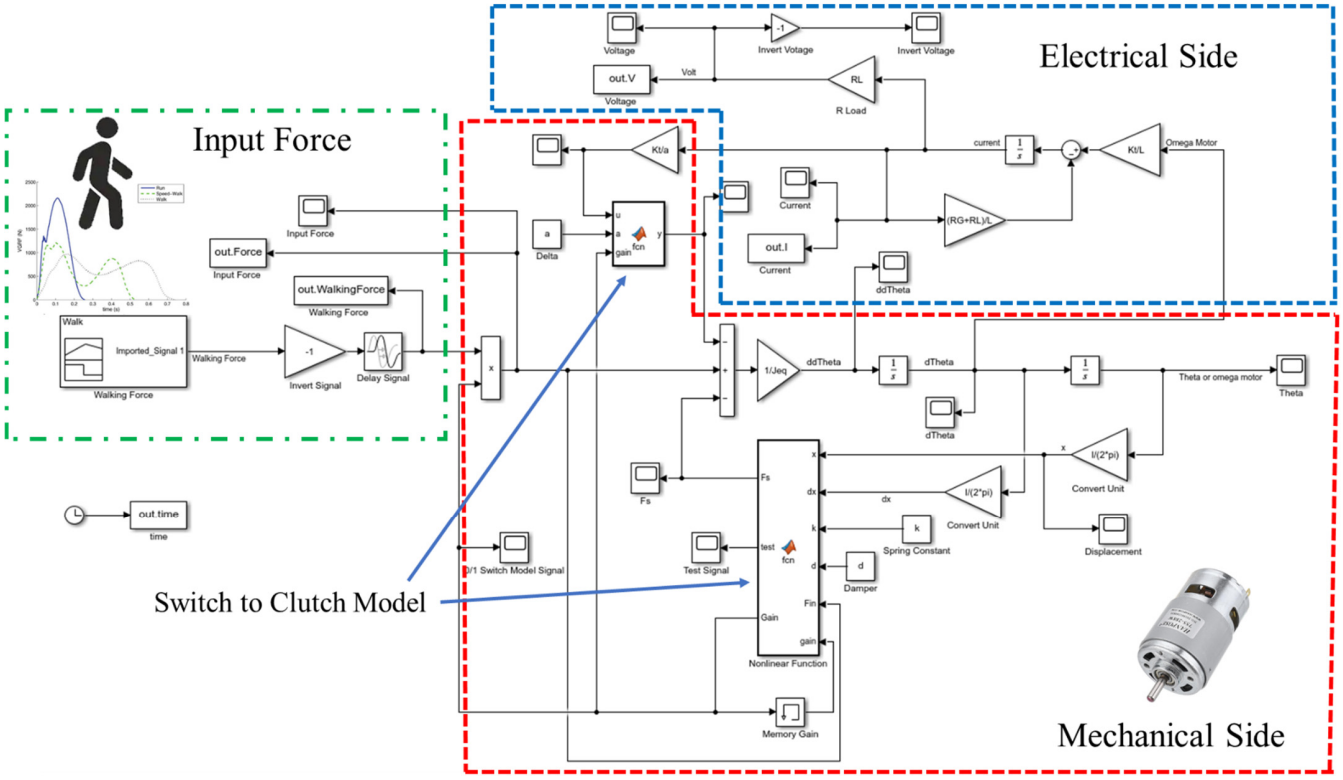

Figure 2. Simulink model for the electromagnetic (EM) generator with lead-screw design and one-way clutch mechanism.

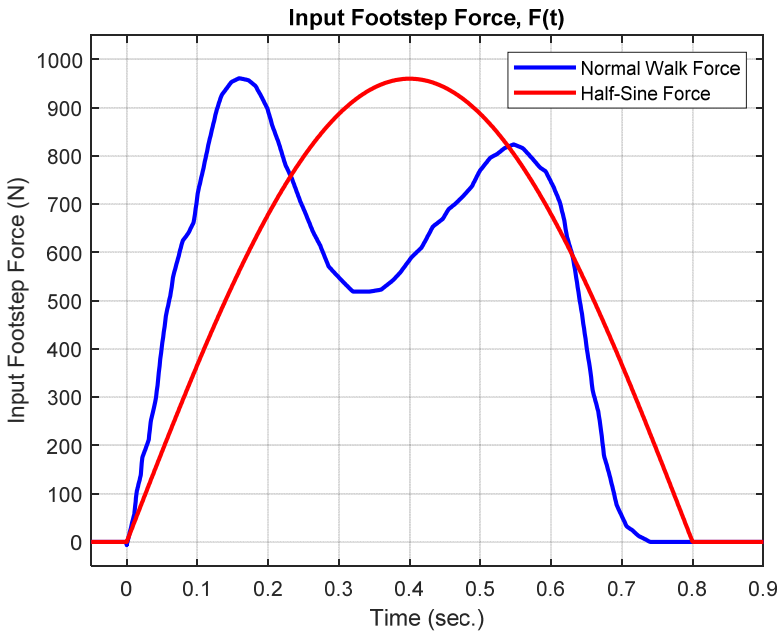

Figure 3. Input footstep force.

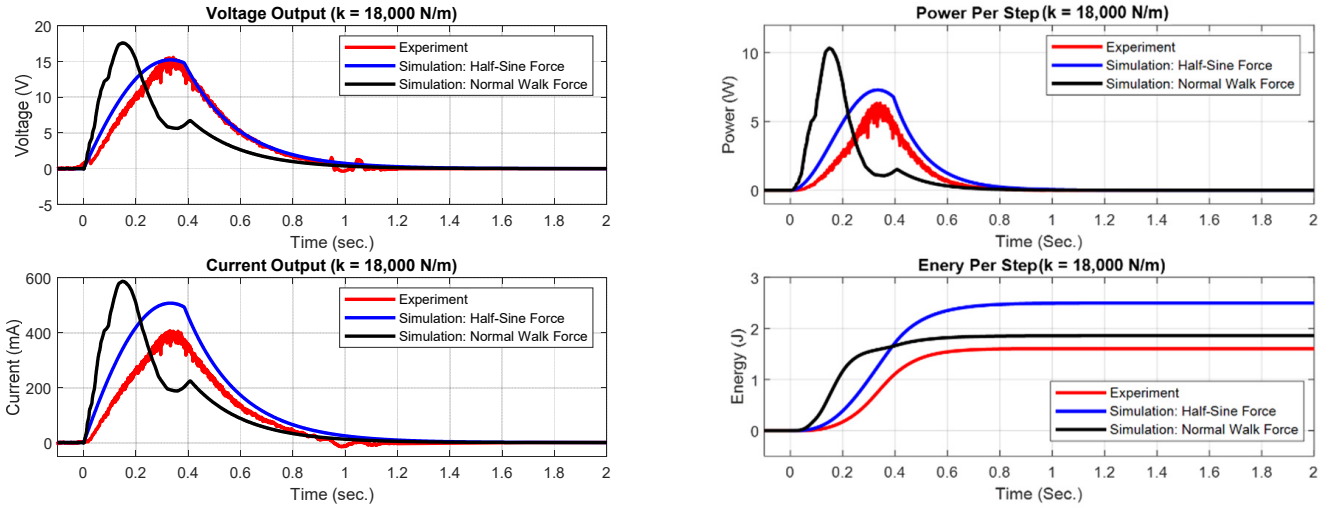

Figure 4. Voltage, current, power, and energy of the Genpath V2 from experiment and simulation: (**a**) voltage and current of the Genpath V2. (**b**) power, and energy of the Genpath V2.

Table 2. Performances of the Genpath V2 when K = 18,000 N/m.

	Experiment	Simulation with Half-Sine Wave Force	Simulation with Normal Walking Force
Variables	**Values per Footstep**	**Values per Footstep**	**Values per Footstep**
Maximum voltage	15.60 V	14.80 V	17.61 V
Average voltage	6.11 V	5.58 V	4.24 V
Maximum current	408.0 mA	493.1 mA	587.1 mA
Average current	154.4 mA	186.0 mA	141.2 mA
Maximum power	6.33 W	7.30 W	10.34 W
Average power	1572 mW	1853 mW	1377 mW
Wave duration	1.02 s	1.35 s	1.35 s
Average energy	1603 mJ	2501 mJ	1859 mJ

Furthermore, the predicted voltage and power/energy harvesting from both the previous design of Genpath V1 [24] and the current design of Genpath V2 with clutch were compared in Figure 5. The prediction of both designs is also compared in Table 3. First, the accumulated energy summarized in Table 3 clearly reveals the improvement of performance of the new design with clutch, which yields total energy of 2501 mJ, i.e., 39% higher than that of the previous Genpath V1. In Figure 5, for the Genpath V1 without clutch, there is the dead zone with no energy gain during 0.4–0.7 s, or when the floor tile reaches the bottom end and stops. Nevertheless, for the design of Genpath V2, when the floor tile reaches the bottom limit, the clutch functions as disengagement, causing the generator rotation continued. Therefore, as seen from the red curves in Figure 5b, there exists additional power to be generated at t > 0.4 s and also more accumulated energy. It is proved that the design concept of the model with clutch significantly helps increase the harvested energy. Another advantage of the design with clutch is to solve the limitation in spring tunning as stated earlier, and it will be discussed in the following section.

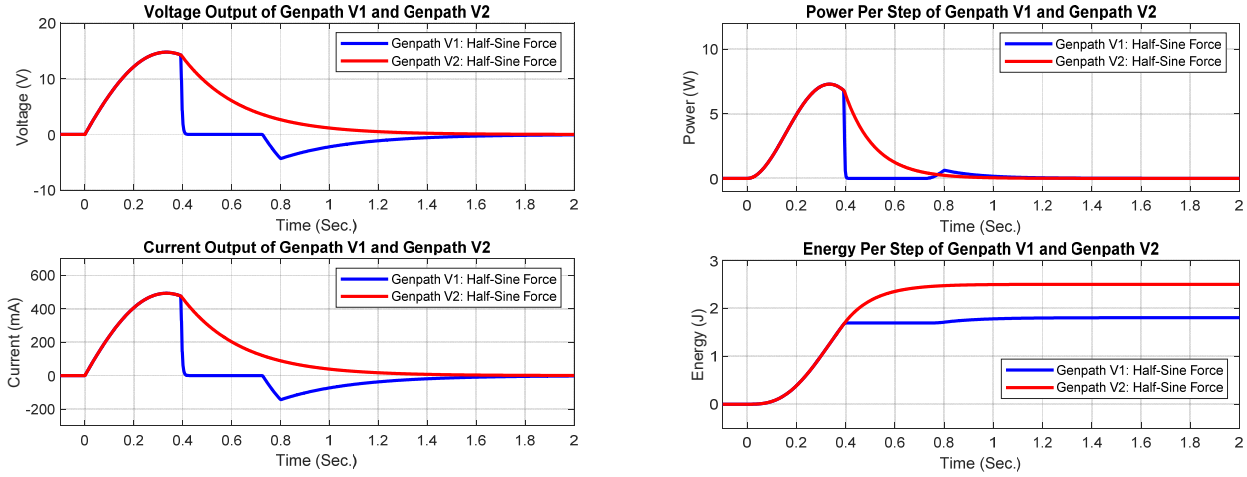

(**a**) (**b**)

Figure 5. Voltage, current, power, and energy of the Genpath V1 and V2 from simulation when K = 18,000 N/m: (**a**) voltage and current of the Genpath V1 and V2. (**b**) power, and energy of the Genpath V1 and V2.

Table 3. Performances of the Genpath V1 and V2 when K = 18,000 N/m.

	Genpath V1 Simulation with Half-Sine Wave Force	**Genpath V2 Simulation with Half-Sine Wave Force**
Variables	**Values per Footstep**	**Values per Footstep**
Maximum voltage	14.78 V	14.78 V
Average voltage	1.93 V	5.377 V
Maximum current	493.2 mA	493.1 mA
Average current	64.3 mA	179.2 mA
Maximum power	7.30 W	7.30 W
Average power	1289 mW	1786 mW
Wave duration	1.40 s	1.40 s
Average energy	1804 mJ	2501 mJ

3.3. Design of Parameters

The analytical model developed in Section 3.2 was used for the selection of optimized parameters. The effect of various mechanical and electrical parameters on the harvested power/energy was investigated. The mechanical parameters are the stiffness coefficient of spring k, the mass of the plate and nut m, and the mass moments of inertia of the lead screw and bevel gear J_1 and J_G. The electrical parameters are the back emf (torque) constant K_t and the resistances of the generator and load R_G and R_L.

3.3.1. Stiffness Coefficient of Spring and Inertias

Figure 6 shows the averaged power when the stiffness coefficient of spring k and the inertia terms, including the mass of the plate and nut m, and the mass moments of inertia of the lead screw and bevel gear J_1 and J_G, are varied, respectively.

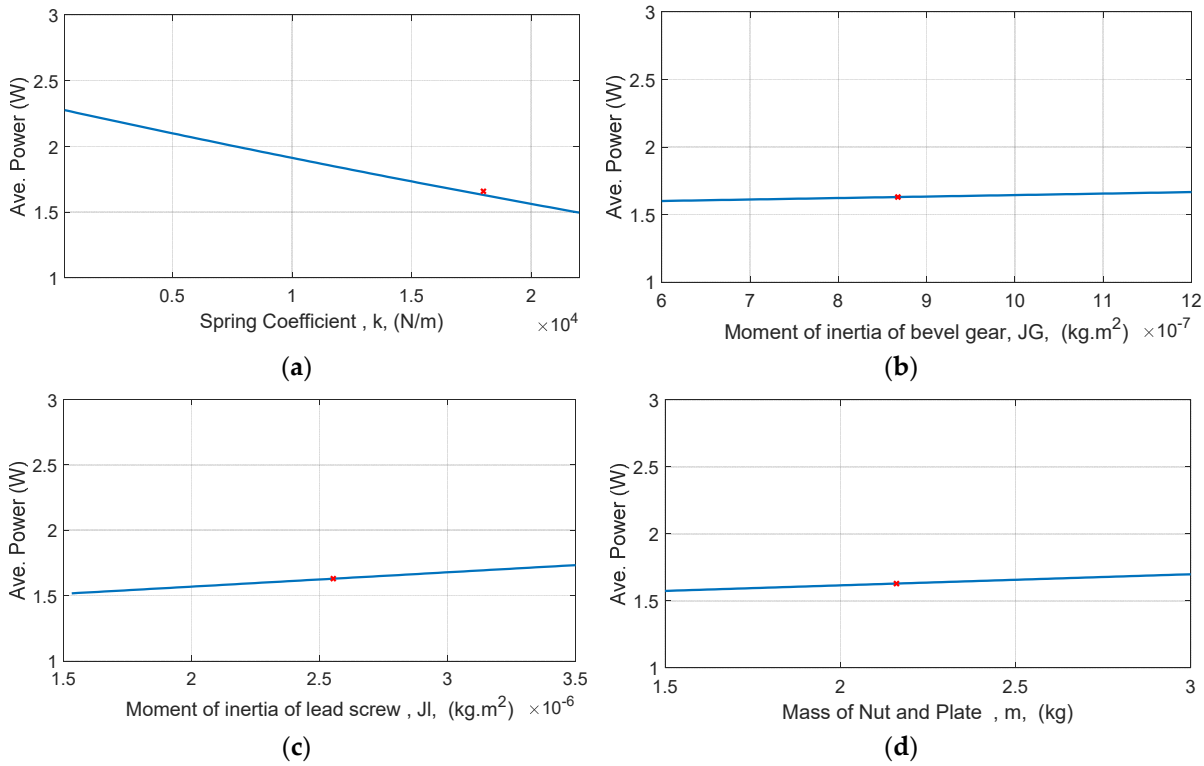

Figure 6. Averaged power when the parameters are varied: (**a**) stiffness coefficient of spring is varied; (**b**) moment of inertia of bevel gear is varied; (**c**) moment of inertia of lead screw is varied; (**d**) mass of nut and plate is varied.

In Figure 6a, the averaged power generated from the energy floor is decreased when the stiffness coefficient is increased. With lower stiffness coefficient k, the velocity of the floor vibration transmitted to the generator shaft is rising, resulting in the increase in the shaft's rotational speed which yields the higher power to be generated. Figure 6a also shows that the stiffness coefficient could be selected much lower than the nominal value of 18,000 N/m to increase the power. Although there is a limitation on using the softer spring in Genpath V1 because of the insufficient restoring force to restore the floor tile back [24], several functional tests with a wide range of softer springs proved no such problem found on the new Genpath V2. When the clutch in the new design is disengaged, the friction torque from the generator is cut-off. Therefore, the restoring force provided by the soft spring still overcomes all the friction from mechanical parts, and is capable of restoring the system back to equilibrium. Consequently, the value of the stiffness coefficient of the springs should be designed as low as possible. However, for durability, the minimum value of an equivalent stiffness coefficient of the coil springs should be ~1500 N/m based on the experiment evaluation of Genpath V2 with the spring stiffness coefficient of 18,000, 3800, 1700, and 760 N/m.

The inertia terms have less effect on the averaged power as seen in Figure 6b–d and Table 4. There is a tiny change in the averaged power when either the mass of the plate and nut m, or the mass moments of inertia of the lead screw and bevel gear J_1 and J_G is varied. Therefore, there is no need for adjusting the inertia parameters to improve the performance of the energy floor.

Table 4. Comparison of power when the parameters are varied.

	Decrease 20%	Decrease 10%	Normal Value	Increase 10%	Increase 20%
Spring Coefficient (k) N/m	14,400	16,200	18,000	19,800	21,600
Power (W)	1.751	1.69	1.6297	1.568	1.5113
% Power Increase/Decrease	+7.44%	+3.70%	0.00%	−3.79%	−7.27%
Moment of inertia of bevel gear (J_G) kg·m^2	6.9400×10^{-7}	7.8075×10^{-7}	8.6750×10^{-7}	9.5425×10^{-7}	10.4100×10^{-7}
Power (W)	1.6107	1.6202	1.6297	1.6392	1.6487
% Power Increase/Decrease	−1.16%	−0.58%	0.00%	+0.58%	+1.17%
Moment of Inertia of lead screw (J_l) kg·m^2	2.0428×10^{-6}	2.2982×10^{-6}	2.5536×10^{-6}	2.8089×10^{-6}	3.0640×10^{-6}
Power (W)	1.5737	1.6018	1.6297	1.6577	1.6858
% Power Increase/Decrease	−3.44%	−1.71%	0.00%	+1.72%	+3.44%
Mass of Nut and Plate (m) kg	1.728	1.944	2.16	2.376	2.592
Power (W)	1.5940	1.6119	1.6297	1.6476	1.6654
% Power Increase/Decrease	−2.19%	−1.09%	0.00%	+1.10%	+2.19%

3.3.2. R_G and K_t

Figure 7 shows the contour plot of the averaged power obtained from the generator when the back emf constant K_t and the internal resistance of the generator R_G are varied. In Figure 7, the generator with greater value of K_t, but smaller value of R_G yields the higher power. However, the value of the back emf constant K_t is naturally proportional to the internal resistance R_G. With the similar plot as Figure 7, one could select the proper type and characteristics of the generator motor to improve the performance of the energy floor.

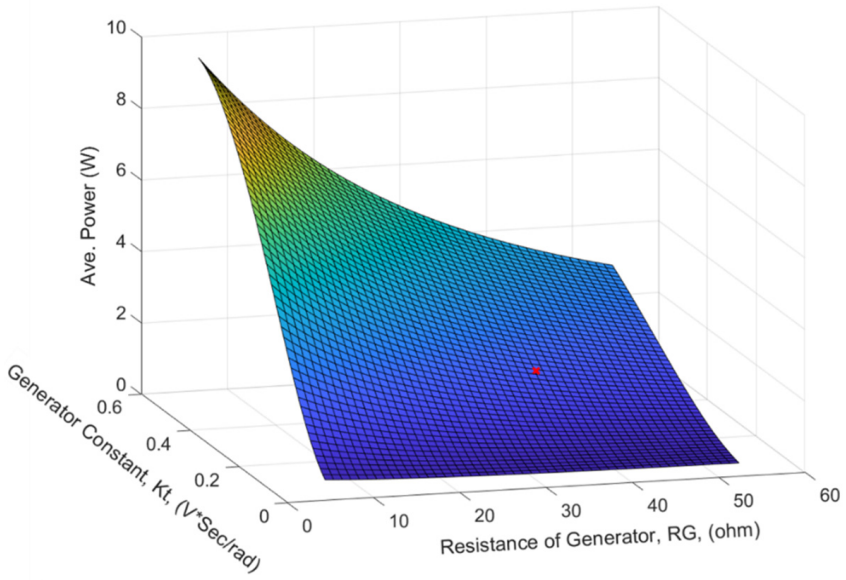

Figure 7. Contour plot of the averaged power when generator constant and resistance of generator are varied.

3.3.3. Optimized Resistive Load R_L

Figure 8 shows the averaged power when the load resistance R_L is varied. It is found that the optimized value of R_L for the highest power is at 41 Ω which is slightly higher than the internal resistance R_G of the generator. The slight difference of R_L and R_G might be because of the compensation of the equivalent mechanical resistance according to the frictional damping as derived in (9). The load resistance R_L of the system can be designed approximately equal to the internal resistance R_G of the generator.

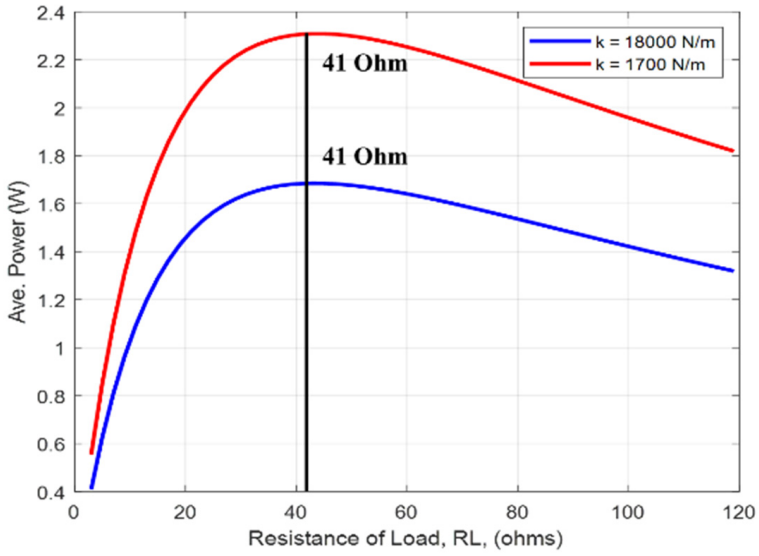

Figure 8. Averaged power when the load resistance is varied.

4. Prototype and Test Results

Figure 9 shows the Genpath V2 built with the key components as listed in Table 5. The major changes of the design were (1) the clutch was installed to the system, and (2) the much softer coil springs with stiffness coefficient of 1700 N/m were selected to replace the springs in the previous model. To perform the performance test, Figure 10 shows the measurement of the voltage across the load resistor R_L and the current i when a normal footstep is applied. Then, the corresponding electrical power and energy were determined from the test results. The experimental results are shown in Figure 11 by the red plots, comparing to the simulation results. It is noted that with the soft spring replacement, the peaks of the induced voltage and current in Figure 11a are much higher than those from the previous prototype, thus the Genpath V2 provides much higher power and energy. Furthermore, Figure 11 also shows the new design with clutch helps extend the interval of energy harvesting after ~0.4 s when the clutch is disengaged. The performance of the Genpath V2 is also summarized in Table 6. The prototype produces an average energy of 3637 mJ (or average power of 3219 mW), per footstep. The energy generated by the new Genpath's prototype was 2935 mJ greater than that of the previous design [24]. With the clutch included in the design, the capability of extending the period of energy harvesting and of increasing the electrical peaks with the softer spring significantly improve the performance.

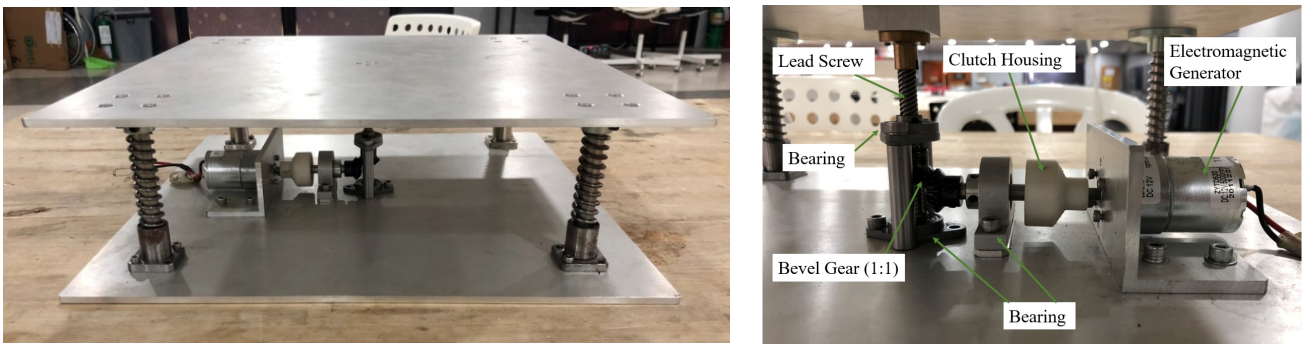

(**a**) (**b**)

Figure 9. Genpath V2 design. (**a**) Photograph of Genpath V2; (**b**) Photograph of Genpaht V2 Mechanism.

Table 5. Parameter of Genpath V2.

Genpath V2		
Item	**Dimensions**	**Number**
Wood plate	400 × 400 × 5 mm	2
Linear guide	Diameter 12 mm Length 90 mm	4
Linear bearing	Inner diameter 12 mm	4
Shaft coupling	Inner diameter 12 mm	4
Coil spring *	Length 60 mm Diameter 2.2 mm	4
Shaft to generator	Diameter 8 mm Length 60 mm	1
Nut and lead screw	Diameter 8 mm Pitch 2 mm	1
Flexible coupling	8 mm	1
Bevel gear	Inner diameter 8 mm	2
Ball bearing	Inner diameter 8 mm	3
Clutch	CSK8 PP	1
Housing	22 × 32 × 29 mm	1
Generator	ZGA37RG 12V 300 rpm	1

* Coil springs are made of difference materials and Genpath V2 with the spring stiffness coefficient of 18,000, 3800, 1700, and 760 N/m have been experimented.

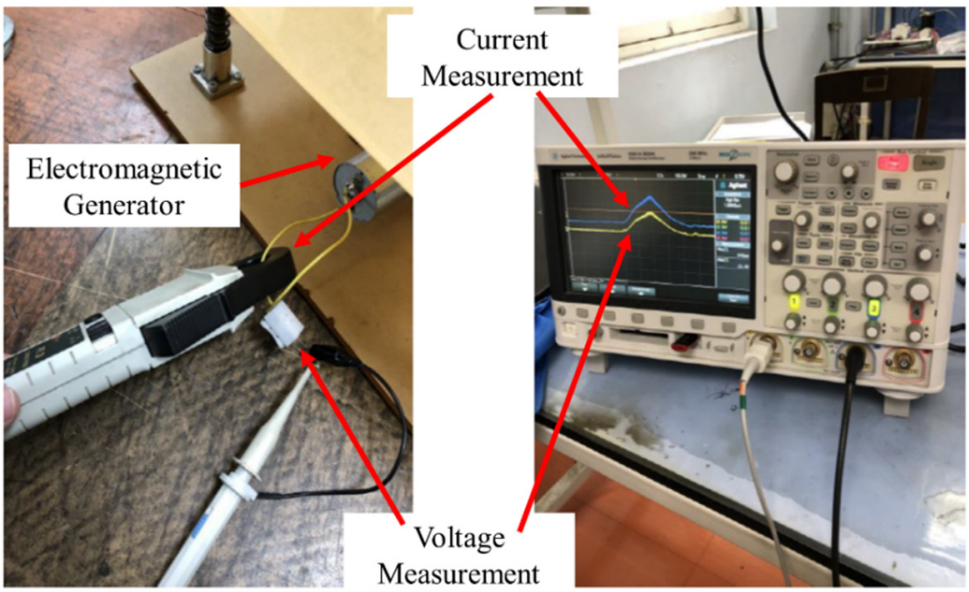

Figure 10. The measurement of the voltage across the load resistor and the current.

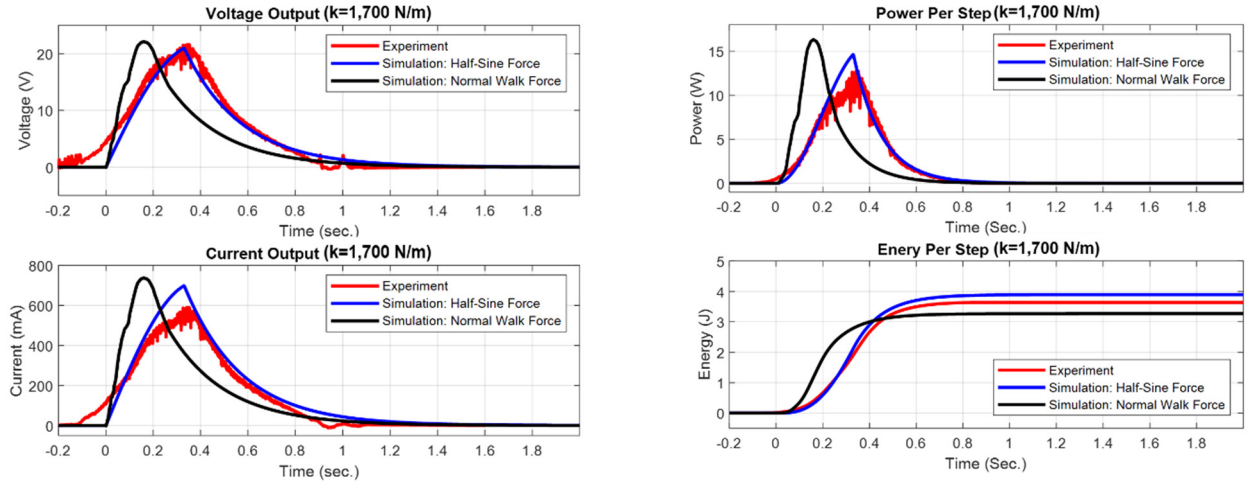

(**a**) (**b**)

Figure 11. Voltage, current, power, and energy of the Genpath V2 from experiment and simulation when K = 1700 N/m: (**a**) voltage and current of the Genpath V2. (**b**) power, and energy of the Genpath V2.

Table 6. Performances of the Genpath V1 [24] and the Genpath V2 when K = 1700 N/m.

Variables	Genpath V1	Genpath V2	Genpath V2	Genpath V2
	Experiment	Experiment	Simulation with Half-Sine Wave Force	Simulation with Normal Walking Force
	Values per Footstep	Values per Footstep	Values per Footstep	Values per Footstep
Maximum voltage	9.5 V	21.60 V	20.95 V	22.12 V
Average voltage	2.88 V	8.59 V	6.53 V	5.376 V
Maximum current	285 mA	590 mA	698.2 mA	737.2 mA
Average current	88 mA	231.1 mA	217.8 mA	179.2 mA
Maximum power	2.71 W	12.74 W	14.62 W	16.31 W
Average power	520 mW	3219 mW	2782 mW	2335 mW
Wave duration	1.35 s	1.13 s	1.40 s	1.40 s
Average energy	702 mJ	3637 mJ	3895 mJ	3269 mJ

5. Power Management System

The power management and storage (PMS) circuit was designed to convert and store electrical energy at the same time. Figure 12 shows the power management and storage. PMS is conducted by a power electronics converter which is comprised of 2 parts: active bridge rectifier and buck-boost converter. Firstly, the AC voltage from generator is rectified by the active-bridge rectifier, the efficiency of this type of rectifier is higher than that of the typical diode-bridge rectifier. Secondly, the buck-boost converter helps to transfer the DC power and charge into a 6V-4.5Ah battery. Lastly, in order to gain the maximum power transfer, the buck-boost converter functions in accordance with the matching-impedance control scheme embedded in the MCU PIC16F1776. The detail of the PMS presents in [24].

In [24], the efficiency of PMS is investigated; the efficiency of active rectifier is 95.78%, the efficiency of buck-boost converter is 78% and the overall efficiency of the PMS is 74.72%. In addition, the power consumption of PMS, from the experimental measurement, is about 94 mW.

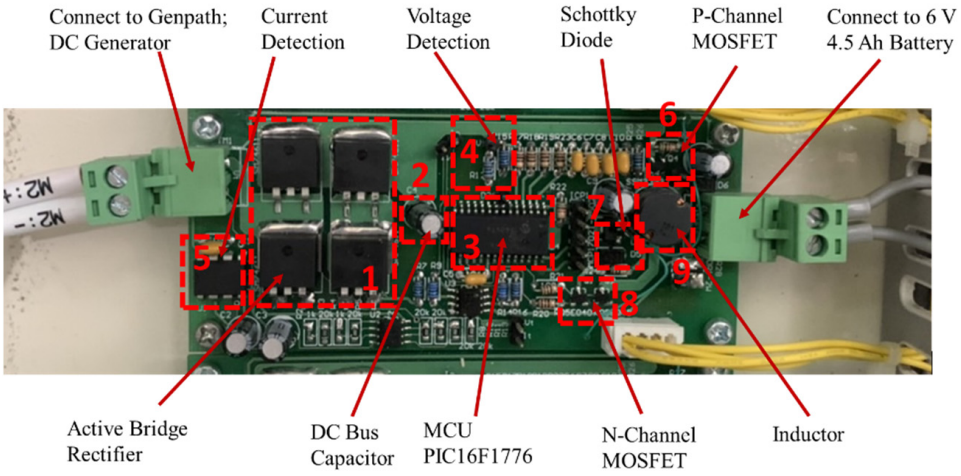

Figure 12. Circuit of power management and storage system.

6. Installation and Exhibition

The purpose of the project is also to raise the social awareness about energy usage as well as the thought of energy harvesting from the environment. To achieve the purpose, there was the exhibition, "Genpath Empower our Journey", arranged during the project. Nine sets of Genpath prototypes with allowable displacement of 10 mm were built and installed for the public exhibition under the slogan "Harness Energy in Every Footsteps". The exhibition is set at the faculty of engineering, Chulalongkorn university, and displays during May to August 2022. Figure 13 illustrates the exhibition environment. Figure 13a shows the Genpath exhibition design drawing. The exhibition was set up in a crowded area and it was not blocking the traffic. The ramp, the Genpath exhibition walkway, was built with the slope of 6 degree and the height of 30 cm for installing the nine sets of Genpath. Thus, the pedestrian is able to comfortably walk on the ramp.

Figure 13d shows the Genpath Exhibition Walkway. The people who stroll forward on the paths can realize how much energy they gain from their footsteps from the display monitors. There are two monitors to display the Genpath Exhibition results. The upper monitor is used to display the exhibition information and give the audient the knowledge and the social awareness about energy usage. Then, the lower monitor is used to display energy results, the energy converting from walking and the total energy collected in a day, as shown in Figure 13b. Moreover, the harvested energy was utilized in the mobile phone charge with the charging terminal shown in Figure 13d. In summary, the benefit of the Genpath is also for a lot of applications, such as a wireless sensor and Internet of Thing applications (IoTs).

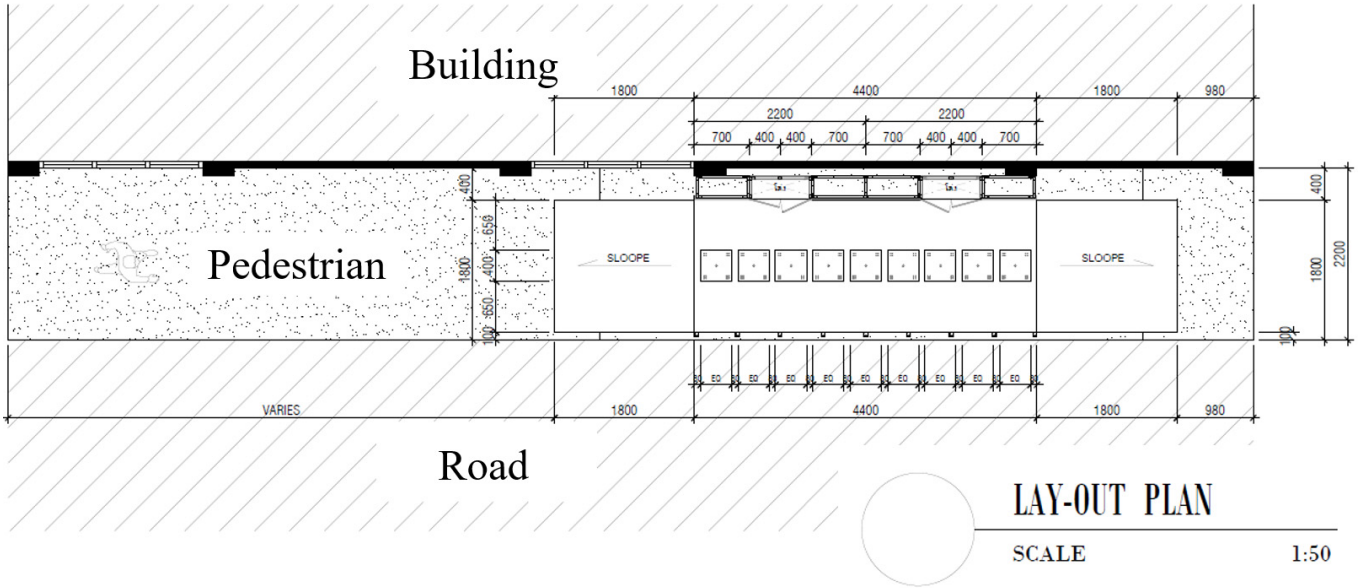

(**a**)

(**b**)

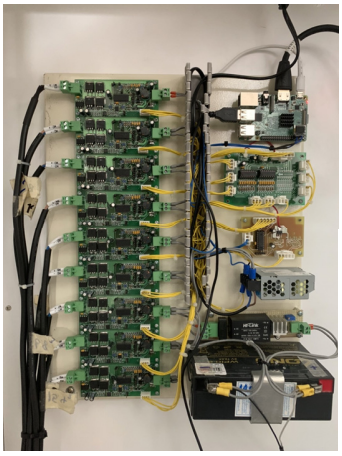

(**c**)

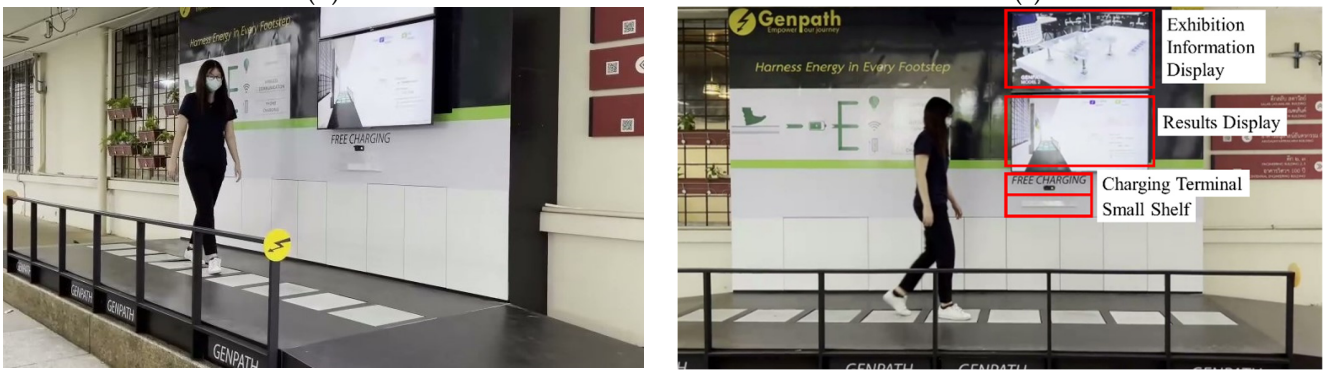

(**d**)

Figure 13. Genpath exhibition, "Genpath empower our journey": (**a**) Genpath exhibition design drawing (**b**) energy result display (**c**) PMS for the exhibition walkway (**d**) Genpath exhibition walkway.

7. Conclusions

The design of the energy floor using the electromagnetic generator is proved to be efficient. The thorough investigation of the design components as well as the dynamic analysis of the system help improve its efficiency. The entire system consists of two main parts of (1) the EM generator, including the lead-screw mechanism for translation-to-rotation conversion, and (2) the Power Management and Storage (PMS) circuit. It was

found that the EM generator shaft in the previous design [24] cannot continuously rotate when the floor-tile reaches the bottom end, resulting in no energy gain. A one-way clutch is implemented to the system to disengage the generator shaft from the lead-screw motion when the floor-tile reaches the allowable displacement. During the disengagement, the EM generator shaft still proceeds a free rotation and generates more power. Moreover, the spring stiffness mainly affects the force transmitted to the EM generator and the induced voltage of the generator, thus the stiffness value is needed to be optimized to increase the harvested power. In our analysis, the dynamic model of the electro-mechanical systems with the one-way clutch was successfully used to predict the energy performances of the VEH floors and fine-tune the design parameters. The new prototype consisting of 12-V-DC generator, mechanisms of lead-screw and clutch, and coil springs with optimal stiffness of 1700 N/m was built and tested. The average energy produced by the new prototype is 3637 mJ (or average power of 3219 mW) per footstep, which is 2935 mJ greater than that of the previous design [24]. Moreover, to raise the social awareness about energy usage, the sets of Genpath have been used to organize an exhibition, "Genpath Empower our Journey". The people who stroll forward on the paths can realize how much energy they gain from their footsteps.

Author Contributions: Conceptualization, T.J., G.P. and S.S.; methodology, T.J., G.P. and S.S.; software, W.T., V.K. and W.W.; validation, T.J., G.P. and S.S.; formal analysis, T.J.; investigation, T.J., W.T., V.K. and W.W.; resources, G.P.; data curation, W.T., V.K. and W.W.; writing—original draft preparation, T.J. and G.P.; writing—review and editing, T.J., G.P. and S.S.; visualization, T.J. and G.P.; supervision, S.S.; project administration, G.P.; funding acquisition, T.J. All authors have read and agreed to the published version of the manuscript.

Funding: This research was funded by Ratchadaphiseksomphot Endowment Fund Chulalongkorn University, grant number CU_GI_63_07_21_01.

Informed Consent Statement: Not applicable.

Data Availability Statement: Not applicable.

Acknowledgments: We would like to thank W. Lowattanamart, V. Suttisung, and S. Sintragoonchai who initiated and supported the idea on the project and built up Genpath prototype-I. Special thanks to CU VISION X and Chulalongkorn University Technology Center for supporting the research innovation eco-system.

Conflicts of Interest: The authors declare no conflict of interest. The funders had no role in the design of the study; in the collection, analyses, or interpretation of data; in the writing of the manuscript; or in the decision to publish the results.

References

1. Pérez, L.; Rodríguez-Jiménez, S.; Rodríguez, N.; Usamentiaga, R.; García, D.F. Digital Twin and Virtual Reality Based Methodology for Multi-Robot Manufacturing Cell Commissioning. *Appl. Sci.* **2020**, *10*, 3633. [CrossRef]
2. Liu, M.; Fang, S.; Dong, H.; Xu, C. Review of digital twin about concepts, technologies, and industrial applications. *J. Manuf. Syst.* **2021**, *58*, 346–361. [CrossRef]
3. Vocca, H.; Cottone, F. Kinetic energy harvesting. In *ICT-Energy-Concepts Towards Zero-Power Information and Communication Technology*; IntechOpen: London, UK, 2014. [CrossRef]
4. Hasan, M. State of IoT 2022: Number of connected IoT devices growing 18% to 14.4 billion globally. *IOT Anal. Mark. Insights Internet Things* **2022**. Available online: https://iot-analytics.com/number-connected-iot-devices/ (accessed on 31 July 2022).
5. Shah, A.S.; Nasir, H.; Fayaz, M.; Lajis, A.; Shah, A. A review on energy consumption optimization techniques in IoT based smart building environments. *Information* **2019**, *10*, 108. [CrossRef]
6. Chalasani, S.; Conrad, J.M. A survey of energy harvesting sources for embedded systems. In Proceedings of the IEEE SoutheastCon 2008, Huntsville, AL, USA, 3–6 April 2008; pp. 442–447. [CrossRef]
7. Akinaga, H. Recent advances and future prospects in energy harvesting technologies. *Jpn. J. Appl. Phys.* **2020**, *59*, 110201. [CrossRef]
8. Jayakumar, H.; Lee, K.; Lee, W.S.; Raha, A.; Kim, Y.; Raghunathan, V. Powering the internet of things. In Proceedings of the 2014 International Symposium on Low Power Electronics and Design, La Jolla, CA, USA, 11–13 August 2014; pp. 375–380.
9. Elahi, H.; Munir, K.; Eugeni, M.; Atek, S.; Gaudenzi, P. Energy harvesting towards self-powered IoT devices. *Energies* **2020**, *13*, 5528. [CrossRef]

10. Dinulovic, D.; Brooks, M.; Haug, M.; Petrovic, T. Rotational electromagnetic energy harvesting system. *Phys. Procedia* **2015**, *75*, 1244–1251. [CrossRef]
11. Weimer, M.A.; Paing, T.S.; Zane, R.A. Remote area wind energy harvesting for low-power autonomous sensors. In Proceedings of the 2006 37th IEEE Power Electronics Specialists Conference, Jeju, Korea, 18–22 June 2006; pp. 1–5.
12. Alippi, C.; Galperti, C. An adaptive system for optimal solar energy harvesting in wireless sensor network nodes. *IEEE Trans. Circuits Syst. I Regul. Pap.* **2008**, *55*, 1742–1750. [CrossRef]
13. Wei, X.; Zhao, Z.; Wang, L.; Jin, X.; Yuan, Z.; Wu, Z.; Lin Wang, Z. Energy conversion system based on Curie effect and triboelectric nanogenerator for low-grade heat energy harvesting. *Nano Energy* **2022**, *91*, 106652. [CrossRef]
14. Jin, X.; Yuan, Z.; Shi, Y.; Sun, Y.; Li, R.; Chen, J.; Wang, L.; Wu, Z.; Lin Wang, Z. Triboelectric Nanogenerator Based on a Rotational Magnetic Ball for Harvesting Transmission Line Magnetic Energy. *Adv. Funct. Mater.* **2022**, *32*, 2108827. [CrossRef]
15. Wu, Z.; Guo, H.; Ding, W.; Wang, Y.; Zhang, L.; Lin Wang, Z. A Hybridized Triboelectric–Electromagnetic Water Wave Energy Harvester Based on a Magnetic Sphere. *ACS Nano* **2019**, *13*, 2349–2356. [CrossRef] [PubMed]
16. Brunner, S.; Gerst, M.; Pylatiuk, C. Design of a body energy harvesting system for the upper extremity. *Curr. Dir. Biomed. Eng.* **2017**, *3*, 331–334. [CrossRef]
17. Choi, Y.M.; Lee, M.G.; Jeon, Y. Wearable biomechanical energy harvesting technologies. *Energies* **2017**, *10*, 1483. [CrossRef]
18. Beeby, S.P.; Torah, R.N.; Tudor, M.J.; Glynne-Jones, P.; O'Donnell, T.; Saha, C.R.; Roy, S. A Micro Electromagnetic Generator for Vibration Energy Harvesting. *J. Micromech. Microeng.* **2007**, *17*, 1257–1265. [CrossRef]
19. Bassett Jr, D.R.; Wyatt, H.R.; Thompson, H.; Peters, J.C.; Hill, J.O. Pedometer-measured physical activity and health behaviors in United States adults. *Med. Sci. Sports Exerc.* **2010**, *42*, 1819. [CrossRef] [PubMed]
20. World Population Prospects 2019. Available online: https://population.un.org/wpp/ (accessed on 31 July 2022).
21. Riemer, R.; Shapiro, A. Biomechanical Energy Harvesting from Human Motion: Theory, State of the Art, Design Guidelines, and Future Directions. *J. Neuroeng. Rehab.* **2011**, *8*, 22. [CrossRef]
22. Energy Floors 2022. Available online: https://energy-floors.com (accessed on 31 July 2022).
23. Pavegen 2022. Available online: https://pavegen.com/ (accessed on 31 July 2022).
24. Jintanawan, T.; Phanomchoeng, G.; Suwankawin, S.; Kreepoke, P.; Chetchatree, P.; U-viengchai, C. Design of Kinetic-Energy Harvesting Floors. *Energies* **2020**, *13*, 5419. [CrossRef]
25. Lowattanamart, W.; Suttisung, V.; Sintragoonchai, S.; Phanomchoeng, G.; Jintanawan, T. Feasibility on development of kinetic-energy harvesting floors. In *IOP Conference Series: Earth and Environmental Science*; IOP Publishing: Bristol, UK, 2020; Volume 463, p. 012107.
26. Liu, M.; Lin, R.; Zhou, S.; Yu, Y.; Ishida, A.; McGrath, M.; Kennedy, B.; Hajj, M.; Zuo, L. Design, Simulation and Experiment of a Novel High Efficiency Energy Harvesting Paver. *Appl. Energy* **2018**, *212*, 966–975. [CrossRef]
27. The MathWorks Inc., Matlab. Available online: https://www.mathworks.com (accessed on 23 April 2022).
28. Stephen, N.G. On Energy Harvesting from Ambient Vibration. *J. Sound Vib.* **2006**, *1–2*, 409–425. [CrossRef]